AD-A066 539 ARMY ELECTRONICS RESEARCH AND DEVELOPMENT COMMAND WS--ETC F/G 4/1
A THEORETICAL INVESTIGATION OF CLOUD/FOG OPTICAL PROPERTIES AND--ETC(U)
FEB 79 R D LOW
UNCLASSIFIED ERADCOM/ASL-TR-0024 NL

1 OF 1
AD
A066539

END
DATE
FILMED
5 - 79
DDC

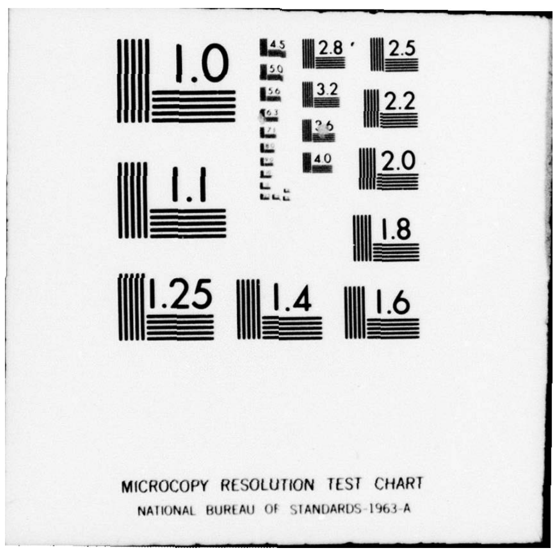
1.0
1.1
1.25
1.4
1.6
1.8
2.0
2.2
2.5
2.8
3.2
3.6
4.0
4.5
5.0
5.6
6.3
MICROCOPY RESOLUTION TEST CHART
NATIONAL BUREAU OF STANDARDS-1963-A

ASL-TR-0024

LEVEL II

AD

Reports Control Symbol
OSD - 1366

(12)

AD A0 66539

A THEORETICAL INVESTIGATION OF CLOUD/FOG OPTICAL PROPERTIES AND THEIR SPECTRAL CORRELATIONS

FEBRUARY 1979

By

RICHARD D. H. LOW

US Army Electronics Research and Development Command
Atmospheric Sciences Laboratory
White Sands Missile Range, NM 88002

NOTICES

Disclaimers

Disposition

(9) Research and development technical rept.,

SECURITY CLASSIFICATION OF THIS PAGE (When Data Entered)

(14) ERADCOM

REPORT DOCUMENTATION PAGE

READ INSTRUCTIONS BEFORE COMPLETING FORM

1. REPORT NUMBER: ASL-TR-0024	2. GOVT ACCESSION NO.
	3. RECIPIENT'S CATALOG NUMBER
4. TITLE (and Subtitle): (6) A THEORETICAL INVESTIGATION OF CLOUD/FOG OPTICAL PROPERTIES AND THEIR SPECTRAL CORRELATIONS.	5. TYPE OF REPORT & PERIOD COVERED: R&D Technical Report
	6. PERFORMING ORG. REPORT NUMBER
7. AUTHOR(s): (10) Richard D. H. Low	8. CONTRACT OR GRANT NUMBER(s)
9. PERFORMING ORGANIZATION NAME AND ADDRESS: Atmospheric Sciences Laboratory, White Sands Missile Range, New Mexico 88002	10. PROGRAM ELEMENT, PROJECT, TASK AREA & WORK UNIT NUMBERS: DA Task Nos. (16) 1T161101A 91A, 1L162111AH 71
11. CONTROLLING OFFICE NAME AND ADDRESS: US Army Electronics Research and Development Command, Adelphi, MD 20783	12. REPORT DATE: (11) Feb[redacted]79
	13. NUMBER OF PAGES: 31
14. MONITORING AGENCY NAME & ADDRESS (if different from Controlling Office): (12) 35p.	15. SECURITY CLASS. (of this report): UNCLASSIFIED
	15a. DECLASSIFICATION/DOWNGRADING SCHEDULE

16. DISTRIBUTION STATEMENT (of this Report)

Approved for public release; distribution unlimited.

17. DISTRIBUTION STATEMENT (of the abstract entered in Block 20, if different from Report)

18. SUPPLEMENTARY NOTES

19. KEY WORDS (Continue on reverse side if necessary and identify by block number)

Cloud/fog models
Liquid water-extinction relationship
Visible
Infrared windows
Spectral correlations

20. ABSTRACT (Continue on reverse side if necessary and identify by block number)

The primary objective of the Electro-Optical Systems Atmospheric Effects Library (EO SAEL) is to provide the Army with an extensive collection of well-conceived and well-documented atmospheric models which can be used with confidence in predicting atmospheric effects on the performances of a variety of electro-optical weapons and communications systems either in computer simulation or under battlefield conditions. One of the models considered is the well-known relationship between visibility (or extinction) and the liquid water content → CONT'

DD FORM 1 JAN 73 1473 EDITION OF 1 NOV 65 IS OBSOLETE

SECURITY CLASSIFICATION OF THIS PAGE (When Data Entered)

410 663

79 03 29 034

20. ABSTRACT (cont)

of a cloud (or fog). However, evidence exists that it varies from one cloud (or fog) to another with different slopes. This paper reexamines this relationship and its ramifications.

Thirty synthetic cloud/fog models were generated by using the gamma and lognormal distribution functions, and their optical properties in the 0.55μm, 1.06μm, 3.75μm, and 10.5μm, calculated according to Mie theory. These 30 models whose liquid water contents ranged from 0.02 to 1.80 g m^{-3} and whose mean radii ranged from 3μm to 12μm should cover, on the average, a wide variety of natural clouds and fogs. The relationship between the visible extinction coefficients and the liquid water contents derived from the models was examined and so were the relationships between the visible and the infrared wavelengths, using available data in the literature and considering sampling errors. Some of the more important findings are given below.

In the case of unimodal or quasi-unimodal drop-size spectra, as can be well-represented by the gamma or the lognormal distribution: (1) visible extinction appears to correlate well with liquid water content and with infrared extinction except when the drop-size spectra are relatively narrow; (2) the consistency of observed microphysical and spectral measurements may be judged by the degree of agreement with the regression lines of the models; (3) by simply increasing or decreasing the liquid water content (or alternately, droplet number concentration), a corresponding change in optical property may be effected without regard to spectral shapes; and (4) sampling errors would cause a much greater error in the calculation of extinction coefficients when large droplets are missing than when small droplets are.

PREFACE

The author expresses his appreciation to Dr. S. G. Jennings, his colleague, and to Dr. James E. Jiusto of the Atmospheric Sciences Research Center, State University of New York at Albany, Albany, New York, for their helpful comments and their critical review of this paper.

CONTENTS

INTRODUCTION

The primary objective of the Electro-Optical Atmospheric Effects Library (EO SAEL) is to provide the Army with an extensive collection of well-conceived and well-documented atmospheric models, which can be used with confidence in predicting atmospheric effects on the performances of a variety of electro-optical weapons and communications systems either in computer simulation or under battlefield conditions. One of the models considered is the well-known inverse relationship between visibility and liquid water content.

The inverse relationship between visibility and the liquid water content of a cloud (or fog), discovered by Trabert [1] and scrutinized by aufm Kampe and Weickmann [2], has been shown to be valid by Houghton and Radford [3] through field measurements and by Eldridge [4] through a "resurrection" of Arnulf and Bricard's [5] haze and fog data. However, as Platt [6] observed, such a relationship is not consistent because its position in a log-log plot shifts in these two studies. The same can also be said of Kumai's [7] data. Reexamining Arnulf and Bricard's [5] measurements in conjunction with Houghton and Radford's [3], Eldridge [4] attributed such inconsistency to the incapability of sampling instruments to depict the complete drop-size spectra.

To measure the complete drop-size distribution is often quite difficult, and two clouds (or fogs) which produce the same visibility may vary in droplet characteristics, depending on their origin, history, and proximity to sources of pollution. These factors serve to mitigate against the formulation of an exact relationship between liquid water content and visibility. As Eldridge [4] pointed out, this relationship will be approximate. Nevertheless, this paper examines this relationship by adopting a different approach in the light of our present knowledge of cloud physics. Instead of using experimental data to elicit such relations, generalized statistical cloud/fog drop distributions shall be constructed encompassing different spectral widths and mean radii so that their liquid water contents and spectral properties at 0.55μm, 1.06μm, 3.75μm, and 10.5μm wavelengths may be calculated exactly. Then experimental data will be used to test the relationship derived between liquid water and spectral extinction. Through this test, the investigation may be able to deduce where the inverse relationship stands in theory, to determine whether visibility can be related to other wavelengths in the infrared, and to clarify factors which may cause this relationship to vary.

GENERATION OF STATISTICAL CLOUD/FOG MODELS

Cloud and fog models have been formulated on the basis of the shapes of drop-size distributions (Carrier et al. [8]; Deirmendjian [9]) and their optical properties investigated. From the cloud physics literature (Fletcher [10]; Borovikov et al. [11]; Jiusto [12]; Mason [13]), apparently liquid water content and mean radius can be used as the central parameters in cloud/fog modeling. From past cloud/fog studies reported in these publications, the following table (table 1) of representative properties may be constructed.

TABLE 1. CLOUD/FOG LIQUID WATER CONTENTS AND MEAN DROPLET RADII

Type	Liquid Water Content ($g\ m^{-3}$)	Mean Radius (μm)
Fogs	0.05 - 0.50	3 - 10
Stratiform Clouds	0.10 - 1.20	4 - 10
Cumuliform Clouds	0.30 - 2.00	5 - 12

In this table, the ranges of liquid water content and mean radius are given for the three general types of clouds (fogs being ground-based clouds). Fogs may vary from radiation through radiation-advection to advection fogs, and stratiform clouds from stratus through stratocumulus to nimbostratus, but in the cumuliform clouds cumulonimbus is excluded because of its inordinately high liquid water content. These ranges are arbitrary and overlapping. Both Borovikov et al. [11] and Mason [13] indicate that statistically the microphysics of these clouds and fogs may well be represented by either a gamma distribution or a lognormal distribution. As will become obvious later, the selection of the distribution function has little bearing on the ultimate spectral properties of clouds.

As a start, synthetic gamma and lognormal distributions were generated so that they span a broad range of spectral widths in terms of their original dispersions, thereby covering liquid water content from about 0.02 $g\ m^{-3}$ to 1.80 $g\ m^{-3}$ and mean radii from 3.0μm through 12.0μm. Furthermore, since not all cloud drop-size spectra share the same size ranges, these synthetic distributions are cut off at different maximum radii.

The probability density function of the gamma distribution is given below:

$$f(r) = \frac{1}{\alpha!\,\beta^{\alpha+1}}\, r^{\alpha} e^{-r/\beta} \qquad (1)$$

where f(r) is the frequency of occurrence of radius r from $r - (1/2)\,\Delta r$ to $r + (1/2)\,\Delta r$, and α and β are the distribution parameters with $\alpha > -1$ and $\beta > 0$. Its principal moments μ_j are

$$\mu_1 = \beta(\alpha + 1) \qquad (2a)$$

$$\mu_2 = \beta^2(\alpha + 1)(\alpha + 2) \qquad (2b)$$

$$\mu_3 = \beta^3(\alpha + 1)(\alpha + 2)(\alpha + 3) \qquad (2c)$$

The mean radius of the distribution R_m, the root-mean-square radius R_s, the mean-volume radius R_v, and the variance σ^2 are given, respectively, by

$$R_m = \mu_1 \tag{3a}$$

$$R_s = \sqrt{\mu_2} \tag{3b}$$

$$R_v = \sqrt[3]{\mu_3} \tag{3c}$$

$$\sigma^2 = \mu_2 - (\mu_1)^2 \tag{3d}$$

Given the mean radius R_m and the liquid water content $W = 4/3\left(\pi R_v^3\right)$ for a spherical water droplet of density equal to 1 g cm^{-3} the distribution parameters α and β can be readily found. But the maximum radius or upper limit of the distribution cannot be specified beforehand since (1) is integrable from 0 to ∞. For the upper limit to be set at a desired value, the frequency of occurrence f(r) at the maximum radius R_{max} must be specified. Noting that the mass of liquid water contained in a 10μm cloud droplet is equivalent to that in 1000 1μm droplets, the following cutoff frequencies are adopted so that there would be little loss of water:

$$f(r) \leq 10^{-4} \text{ for } R_{max} = 15\mu m \text{ and } 20\mu m,$$

and

$$f(r) \leq 10^{-5} \text{ for } R_{max} = 30\mu m, 40\mu m, \text{ and } 50\mu m.$$

Now that both R_m and f(r) are known, (1) can be solved by means of successive approximation simultaneously with (3a) for α and β, putting r = maximum radius.

The probability density function of the lognormal distribution is given by

$$f(r) = \frac{1}{r\log_e\sigma_g\sqrt{2\pi}} \exp\left[-(\log_e r - \log_e r_g)^2/2\log_e^2\sigma_g\right] \tag{4}$$

where r_g and σ_g are the geometric mean and geometric standard deviation, respectively. Let $\mu_x = \log_e r_g$ and $\sigma_x = \log_e \sigma_g$; then, the principal moments of the distribution are:

$$\mu_1 = \exp(\mu_x + \sigma_x^2/2) \quad (5a)$$

$$\mu_2 = \exp(2\mu_x + 2\sigma_x^2) \quad (5b)$$

$$\mu_3 = \exp(3\mu_x + 9\sigma_x^2/2) \quad (5c)$$

Again, the mean radius, the root-mean-square radius, the mean-volume radius, and the variance are given by (3a) - (3d) through (5a) - (5c). Instead of using (4), the following two equations,

$$\log_e R_m = \mu_x + \sigma_x^2/2 \quad (6)$$

$$\log_e R_{max} = \mu_x + 4\sigma_x \quad (7)$$

are solved simultaneously for μ_x and σ_x and hence r_g and σ_g.

Altogether 30 complete synthetic distributions with micrometer interval resolution were generated. Note that even within each size range, standard deviations are somewhat different, signifying different spectral widths within a size range. The distribution parameters together with standard deviation σ, mean radius R_m, and liquid water content W (of 100 droplets cm^{-3}) for each case are shown in table 2. The table as a whole should be adequate to encompass most clouds and fogs when their drop-size spectra are unimodal or quasi-unimodal.

OPTICAL PROPERTIES AND SPECTRAL CORRELATIONS

The volume extinction coefficients β_{ext} at a wavelength is related to the drop-size distribution (van de Hulst [14]; Deirmendjian [9]) by

$$\beta_{ext} = N\pi \int_{r\ min}^{r\ max} Q_{ext}(\lambda,m,r) r^2 f(r) dr \quad (8)$$

TABLE 2. GAMMA AND LOGNORMAL DISTRIBUTION PARAMETERS IN DIFFERENT RADIUS RANGES.

Ranges (μm)	Gamma Distribution					Lognormal Distribution				
	α	β	σ (μm)	R_m (μm)	W ($g\ m^{-3}$)	R_g	σ_g	σ (μm)	R_m (μm)	W ($g\ m^{-3}$)
0 - 15	1.697	1.113	1.83	3.0	0.027	2.752	1.515	1.29	3.0	0.019
	1.509	1.594	2.52	4.0	0.066	3.781	1.399	1.38	4.0	0.038
	6.968	0.628	1.77	5.0	0.074	4.814	1.317	1.40	5.0	0.066
0 - 20	1.509	1.594	2.52	4.0	0.067	3.669	1.519	1.75	4.0	0.045
	2.885	1.287	2.53	5.0	0.099	4.693	1.428	1.84	5.0	0.076
	4.778	1.040	2.50	6.0	0.143	5.725	1.358	1.88	6.0	0.120
0 - 30	1.273	2.640	3.98	6.0	0.243	5.493	1.522	2.63	6.0	0.153
	2.063	2.285	4.00	7.0	0.312	6.519	1.458	2.74	7.0	0.220
	2.980	2.010	4.00	8.0	0.401	7.548	1.406	2.80	8.0	0.303
0 - 40	1.115	3.783	5.50	8.0	0.602	7.323	1.524	3.52	8.0	0.364
	1.656	3.400	5.54	9.0	0.735	8.345	1.475	3.63	9.0	0.479
	2.300	3.040	5.52	10.0	0.874	9.375	1.433	3.71	10.0	0.616
0 - 50	0.996	5.010	7.08	10.0	1.189	9.148	1.525	4.41	10.0	0.713
	1.402	4.580	7.10	11.0	1.413	10.176	1.492	4.58	11.0	0.904
	1.395	5.010	7.75	12.0	1.802	11.201	1.450	4.61	12.0	1.093

or

$$\beta_{ext} = N\pi \sum_{i}^{n} Q_{ext}(\lambda,m,r_i)\ f_i r_i^2 \text{ (per unit interval)}\ , \qquad (9)$$

where Q_{ext} (λ,m,r) is the efficiency factor for extinction, a function of wavelength λ, complex refractive index m, and radius r; f(r) or f_i the distribution frequency; and N the total number density taken to be 100 per unit volume for ease of scaling. Calculations of the volume extinction coefficients were made at four wavelengths (0.55µm, 1.06µm, 3.75µm, and 10.5µm) without considering water vapor absorption, which is negligible in comparison with scattering and absorption by water droplets in a cloudy atmosphere.

Figure 1 is a plot of the liquid water contents in g m^{-3} of all 30 distributions against the corresponding extinction coefficients in km^{-1} at 0.55µm. The regression line was drawn on the basis of a least-square fit which gives a correlation coefficient of 0.997. The regression equation is

$$\beta_{0.55} = 93.2\ W^{0.638}\ km^{-1}. \qquad (10)$$

Then the volume extinction coefficients at 0.55µm were plotted versus those at 3.75µm and at 10.5µm, as shown in figs. 2 and 3, respectively. The former has a correlation coefficient of 0.999, and the regression equation is

$$\beta_{3.75} = 1.487\ \beta_{0.55}^{0.928}\ km^{-1}\ , \qquad (11)$$

The latter has a correlation coefficient of 0.997, and the regression equation is

$$\beta_{10.5} = 0.211\ \beta_{0.55}^{1.378}\ km^{-1}. \qquad (12)$$

Correlation between the two wavelengths of 0.55µm and 1.06µm was not considered since in all cases examined the extinction coefficients at 1.06µm are always larger than those at 0.55µm, but never by more than 4 percent. This may be inferred from fig. 4 which is a plot of extinction coefficients as a function of individual droplet radii, which cover the range of interest. The positive (or inverse) relationship between extinction (or visibility) and liquid water appears to be independent of the shape of a unimodal drop-size distribution.

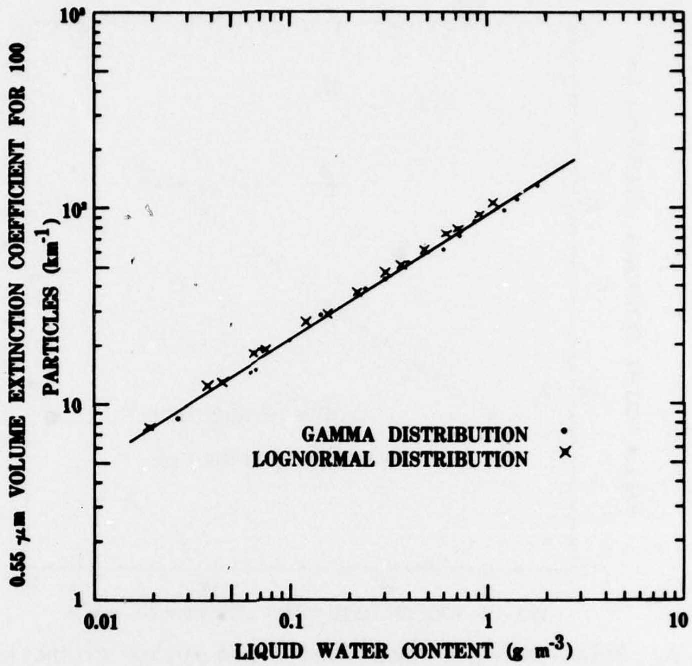

Figure 1. Relationship between visible extinction and liquid water content derived from the gamma and the lognormal distributions given in table 2. The line is a least-square fit.

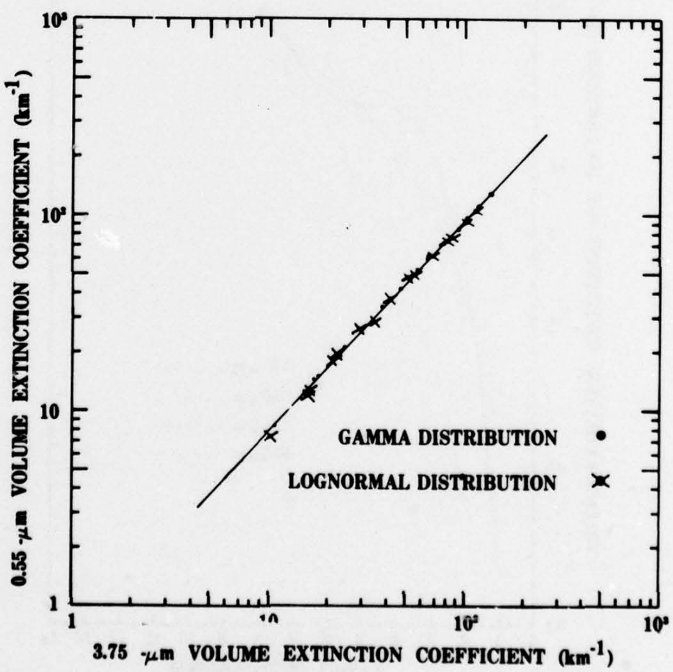

Figure 2. Relationship between 0.55μm and 3.75μm extinction. The line is a least-square fit.

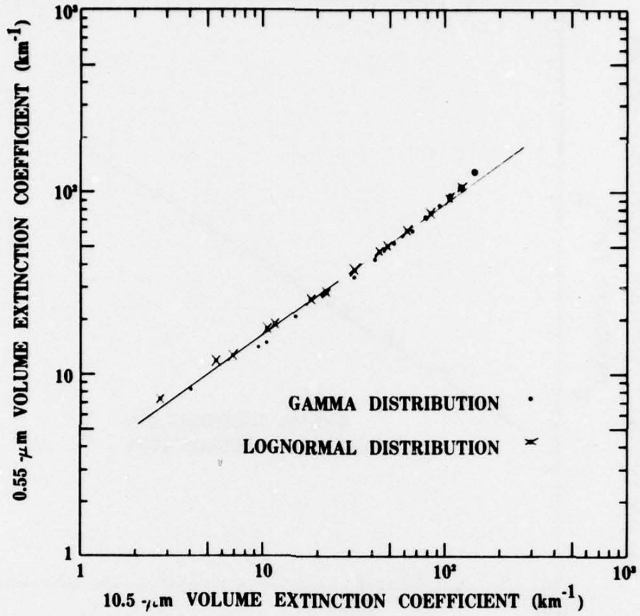

Figure 3. Relationship between 0.55μm and 10.5μm extinction. The line is a least-square fit.

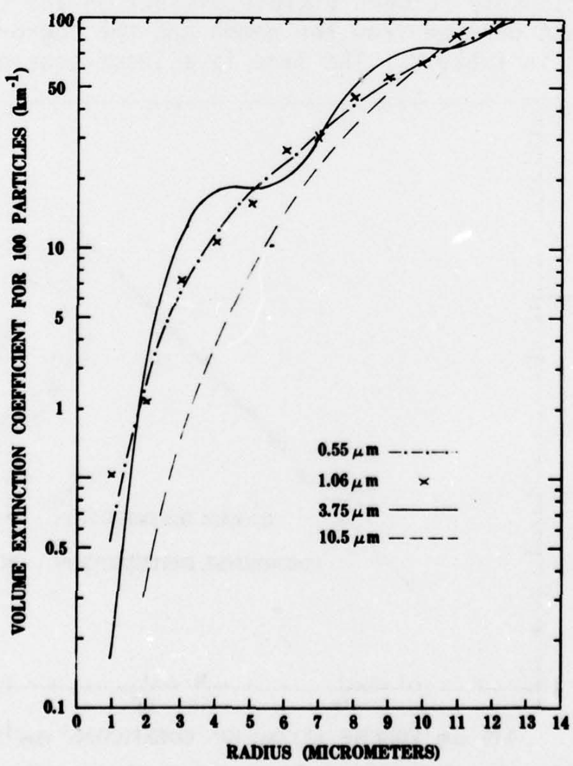

Figure 4. Volume extinction at 0.55μm, 1.06μm, 3.75μm, and 10.5μm wavelengths as a function of droplet radius.

THEORY AND APPLICATIONS

There is excellent correlation between liquid water and extinction for the gamma and lognormal droplet distributions. It is customary to set $Q_{ext} = 2$ for the visible region in a cloudy or foggy environment (Johnson [15]). Then (9) becomes

$$\beta_{ext} = 2N\pi r_s^2 \qquad (13)$$

where r_s, as already defined, is the root-mean-square radius. To express the extinction coefficient as a function of liquid water content, simply divide (13) by $4/3(N\pi r_v^3)$ and multiply it by the same quantity W to yield

$$\beta_{ext} = 1.50\ (r_s^2/r_v^3)\ W \qquad (14)$$

where r_v, as already noted, is the mean-volume radius. Equation (14) when substituted into the Koschmieder expression ($V = 3.912/\beta$) yields the well-known Trabert formulation.

In view of fig. 1, the factor (r_s^2/r_v^3) will correlate just as well with the extinction coefficient. Instead, let $X = r_s^2/r_v^3$ for the gamma distribution and $Y = r_s^2/r_v^3$ for the lognormal distribution, and determine if X and Y are correlated. To do so, we find

$$X = 1/\beta(\alpha + 3) \qquad (15)$$

from (2b) and (2c), and

$$Y = \exp[-(\mu_x + 5\sigma_x^2/2)] \qquad (16)$$

from (5b) and (5c). The relationship of their reciprocals, usually referred to as effective radii, is shown in fig. 5, and the correlation coefficient is 0.987. When the spectra are narrow, there is a greater scatter. In fact, as the drop-size spectrum broadens, the gamma distribution approaches the lognormal distribution, or vice versa, as Levin [16] has shown. Since X and Y appear to behave in a reasonably orderly manner, it is not difficult to infer that the same approach may be used to demonstrate the correlation of the extinction coefficients at 3.75μm and at 10.5μm with liquid water content and hence with the extinction coefficients at 0.55μm.

Since fig. 1 indicates a positive relationship between cloud extinction and cloud liquid water content independent of the shapes of drop-size spectra, it would be of great interest to examine if such a relationship is applicable to real microphysical and visibility data, mindful that not all cloud drop-size spectra are unimodal and that such data may not represent the complete spectra. Unfortunately, few authors presented a tabulation of their data in the literature and even fewer measured liquid water content independently. After a careful survey of the drop-size spectra in the literature, it was decided to take those from Houghton and Radford [3] and the tabulated values of Eldridge [4], Garland [17], and Mack and Pilié [18]. Visibility values were converted to extinction coefficients by means of the well-known Koschmieder formula, as given by Middleton [19]:

$$\beta_{ext} = 3.912/V \tag{17}$$

Where V in kilometers is the meteorological range or simply visibility.

Among the authors referenced, only Houghton and Radford [3] made independent measurement of the liquid water contents in their fogs. Their investigations represent the earliest known attempt to verify the inverse relationship between visibility and liquid water content. Only the values labeled with the symbol "+" were extracted from their fig. 9. Tabulation is not the reason for choosing Eldridge's [4] reconstructed data; the real reason was his imaginative interpretation [20] of the discrepancies between his regression line and Houghton and Radford's [3]. Garland [20] presented both observed and calculated visual ranges in his table, and his observed values were used. The usual practice in the literature to find visibility is by means of (9) and (17) where Q_{ext} is approximated by 2. Instead of following this practice, Mack and Pilié [18] used the following expression:

$$W = \frac{2.6}{V} \frac{\sum_i^N n_i r_i^3}{\sum_i^N n_i r_i^2} , \tag{18}$$

given by aufm Kampe and Weickmann [2], to derive liquid water contents from independent visibility measurements.

Those data were plotted in fig. 6, over which the theoretical or generalized regression line from fig. 1 was reproduced. However, because of their close proximity, quite a few data points clustering around the line were ignored. The two light lines on either side of the regression line represent 15 percent and 50 percent deviations. Except for Eldridge's [4] and some of Garland's [17] data, most points lie within the 50 percent boundaries.

Optical measurements at several wavelengths in cloud or fog conditions are difficult to make successfully. Even more difficult is the determination of the degree of agreement between optical and other microphysical measurements. Arnulf and Bricard [5] merely noted such agreement in their

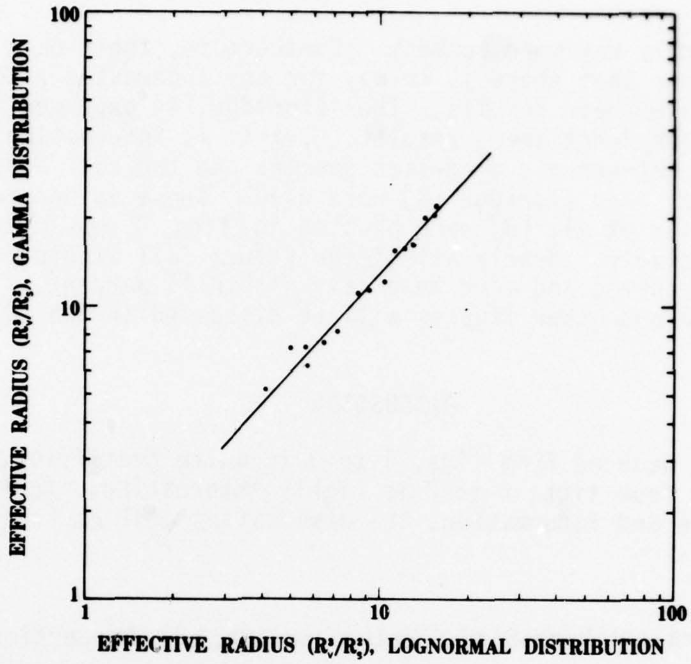

Figure 5. Relationship between effective radii of the gamma and of the lognormal distributions.

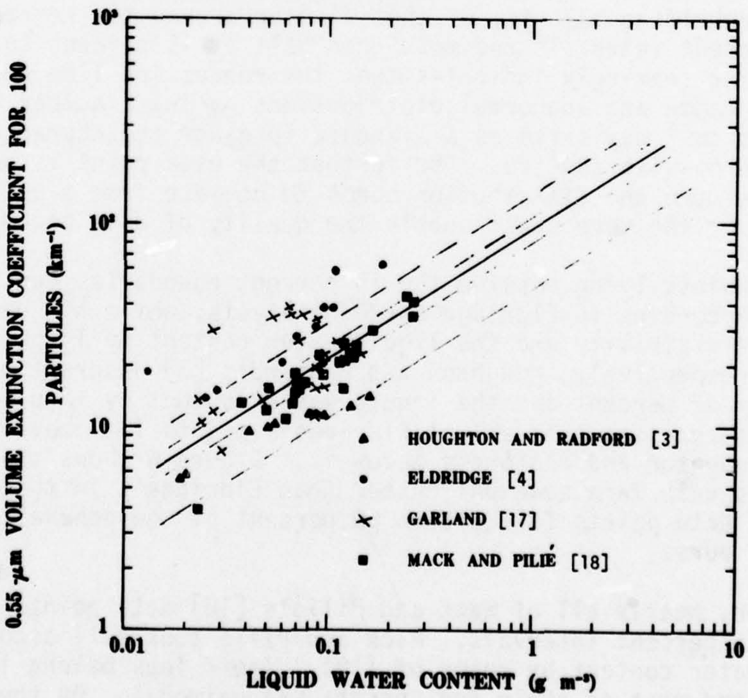

Figure 6. Data from several sources showing the relationship between visible extinction and liquid water content, as compared to the regression line derived in fig. 1. Light dashed lines on either side of the line show 15 percent and 50 percent deviations.

paper with hardly any more comment. Furthermore, their data were presented in such a manner that there is no way for any interested readers to accurately reproduce their results. Thus Eldridge [4] expended a great deal of effort to resurrect these results. But it is interesting to note the discrepancies between his drop-size spectra and theirs. Nonetheless, the spectral values from Eldridge [4] were used. These values together with those of Carrier et al. [8] were plotted in figs. 2 and 3 to produce figs. 7 and 8, respectively. Nearly all of the values fall within 50 percent of the model fog curves and more than half within 15 percent. The implications of these and other figures will be discussed in the following section.

DISCUSSION

The knowledge deduced from figs. 1 to 3 is quite gratifying, and the information gained from figs. 6 to 8 is highly interesting. To further exploit such knowledge and information, the discussions will be separated into three areas.

Equivalent Drop-Size Spectra and Spectral Properties

Although a number of the data points in fig. 6 may have come from bimodal or multimodal distributions and the drop-size spectra may have been imprecise, an overwhelming majority of them cluster around the regression line at the 50 percent intervals and more than half at 15 percent intervals. This clustering seemingly indicates that the regression line derived from the combined gamma and lognormal distributions having a number density of 100 particles cm^{-3} may serve as a standard to gauge the characteristics of observed drop-size spectra. The further the data point is away from the line, the more the distribution seems to deviate from a unimodal distribution or the more questionable the quality of data becomes.

Many of the points lying outside the 15 percent boundaries can be readily explained. According to Eldridge's [20] analysis, while his data underestimated the visibility and the liquid water content by 14 percent and 35 percent, respectively, Houghton and Radford's [3] underestimated the visibility by 42 percent and the liquid water content by 12 percent. It is thus not surprising that all of Eldridge's points lie above the line and all of Houghton and Radford's below it. Figure 6 shows that Houghton and Radford's data fare somewhat better than Eldridge's in that most of the former's data points fall within 50 percent of the generalized regression line of ours.

By comparison, nearly all of Mack and Pilié's [18] data points fall within the 15 percent intervals. Mack and Pilié took full account of the liquid water content by means of (18). Their fogs belong in the radiation type, and most of their fog spectra are unimodal. On the other hand, more than a half of Garland's [17] fogs are of the advection type, and perhaps about a third bimodal, as may be inferred from the few histograms he chose to present. Moreover, as many as five fogs may contain ice

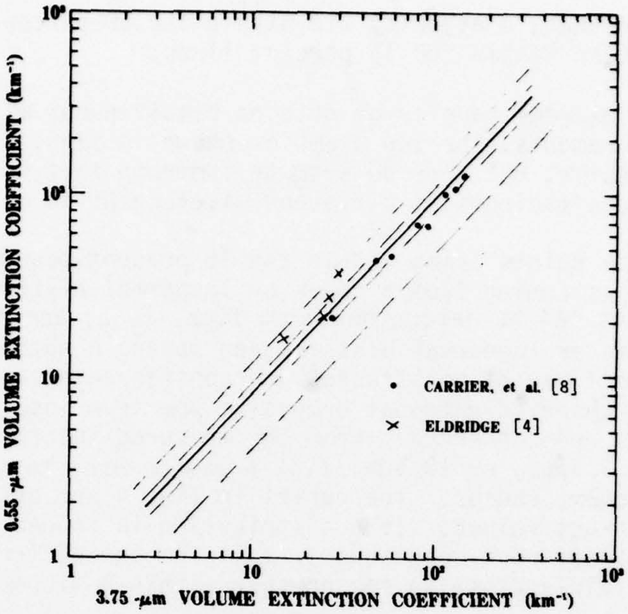

Figure 7. Data from Eldridge [4] and Carrier et al. [8] showing the relationship between 0.55μm and 3.75μm extinction as compared to the regression line derived in fig. 2. Light dashed lines on either side of the line give 15 percent and 50 percent deviations.

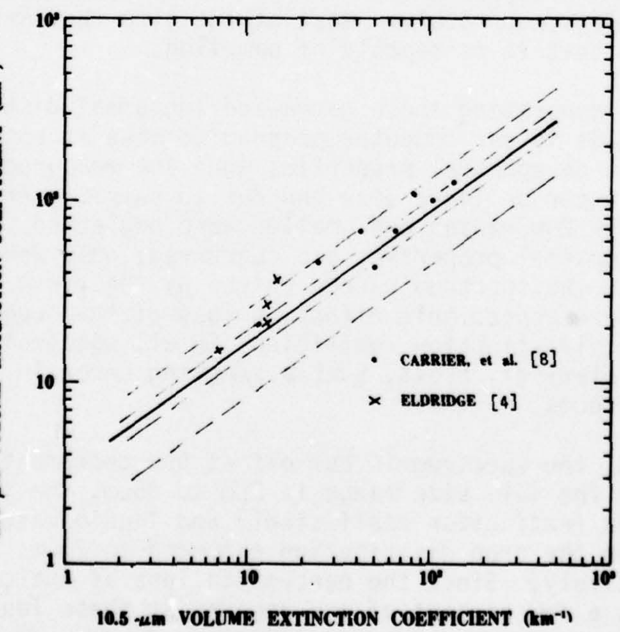

Figure 8. Data from Eldridge [4] and Carrier et al. [8] showing the relationship between 0.55μm and 10.5μm extinction, as compared to the regression line derived in fig. 3. Light dashed lines on either side of the line give 15 percent and 50 percent deviations.

crystals. Despite that, a majority lie within the 50 percent lines and about a half of those within the 15 percent lines.

Since there is an extreme paucity of data on simultaneous microphysical and spectral measurements, the two examples shown in figs. 7 and 8 are not meant to be conclusive, but they do seem to indicate that correlation between extinction coefficients at different wavelengths is quite respectable.

Therefore, any data points lying within the 15 percent boundaries in fig. 6 could be regarded as coming from a gamma or lognormal distribution, and their spectral properties can be determined from figs. 1, 2, and 3. Furthermore, an equivalent gamma or lognormal distribution having a number concentration of 100 droplets cm^{-3} may be constructed and considered a satisfactory substitution for the observed unimodal drop-size spectrum insofar as its optical properties are concerned. From the measured spectral extinction values at 0.55μm, 3.75μm, or 10.5μm, fig. 4 may be used to find the equivalent root-mean-square radius. The curves in fig. 4 are only a smoothed approximation to exact values. If a distribution is indeed gamma or lognormal, the equivalent root-mean-square radii for the different spectral regions will lie fairly close to one another within a micrometer interval.

An Examination of Droplet Sampling Errors

A mechanical droplet impactor is inefficient in capturing small droplets below the 1μm or 2μm radius, and an optical sampling device cannot always count larger droplets accurately. Most of the time the sampling device has a cutoff size that it is capable of sampling.

In the process of generating these gamma and lognormal distributions, provisions were made in our computer program to make it possible to examine the effect on spectral properties when the measured spectrum is truncated in the upper or lower size end due to sampling errors. At the lower end, droplets 2μm radius and smaller were neglected. Insofar as the cloud or fog optical properties are concerned, only when the size range is small and the spectrum narrow (given by the first three lines in table 2) is there appreciable effect, a loss of the order of 10 to 30 percent in the total extinction coefficient in all spectral regions. When the spectrum is relatively broad, such a sampling error in the lower end has negligible effects.

For the upper end, the spectrum is cut off at 5μm decrement intervals. For example, when the full size range is 0μm to 30μm, the losses of optical properties (extinction coefficient) and liquid water content were examined when the drop distribution extended to 25μm, 20μm, 15μm, and 10μm, respectively. Since the percentage loss of optical properties is usually within a few percent of one another at these four wavelengths, fig. 9 may represent any of these wavelengths. In this figure, each complete curve begins at the maximum radius, hence incurring no loss. For each additional 5μm decrement, there is an increasing loss. Take the 0μm to 40μm gamma distribution as an example, the visible extinction coefficient being 84.83 km^{-1}. If our sampling device can pick up droplets no larger than 30μm radius, then there will be a maximum loss of about 4 percent in optical property, i.e., 81.44 km^{-1}. If the device can go up to 15μm only, then the maximum loss will be about 58 percent, or 35.63 km^{-1}. When the droplet spectrum becomes narrower, for the same size range, the loss is a few percent less. Figure 10 is presented in the same vein, except that the loss of liquid water content was plotted versus the loss of optical property. Some uncertainties exist when the drop-size spectra are narrow, but as the spectra broaden, a definitive correlation emerges between these losses; a 20 percent loss of liquid water means a loss of extinction by about 12 percent. The loss of liquid water content as a result of sampling errors in the upper end can be readily deduced from figs. 9 and 10 together, given spectral measurements.

Some Thoughts on Bimodal Distributions

In the cloud physics literature, little attention has been paid to the existence of bimodal droplet distribution in clouds and fogs. One reason is that it is not a common occurrence, as may be seen from the droplet spectra of clouds displayed in cloud physics books (e.g., Fletcher [10]; Borovikov et al. [11]; Mason [13]), and another reason is that the usual statistical practice in experimental work to average several independent samples serves to smooth out drop-size irregularities. Nonetheless, there is evidence that despite the averaging process orographic clouds (e.g., Squires [21]) and coastal low-hanging stratus clouds and fogs (e.g., Ludwig and Robinson [22]) are often bimodal or multimodal. Furthermore, Eldridge [23], using an optical sampling device to measure drop-size distributions in an advection fog (which he called cloud) over a mountain top, showed that in all cases the spectra were bimodal, an inordinately large number of particles (which may not be true cloud droplets at all) at and below 1.5μm radius. Considering the high winds of 9 to 18 m s^{-1} in which the samples were taken, such a large number of small particles may not be too surprising.

In a polluted environment as in the Los Angeles area and other industrial cities, the fogs or low clouds may be expected to display bimodal or sometimes multimodal spectra. Inferences may be drawn from studies made by Whitby and Sverdrup [24] of California aerosols. A large number of tiny solid and gaseous pollution particles together with haze particles would be superimposed upon cloud or fog droplets, thereby giving rise to bimodal or multimodal distributions.

CONCLUSIONS

On the basis of the gamma and lognormal distributions, 30 synthetic cloud/fog models were analyzed optically. These 30 models cover a wide range of spectral widths and liquid water contents, and thus embrace most clouds and fogs in nature. These distributions are believed to represent reasonably well cloud and fog data found in the literature.

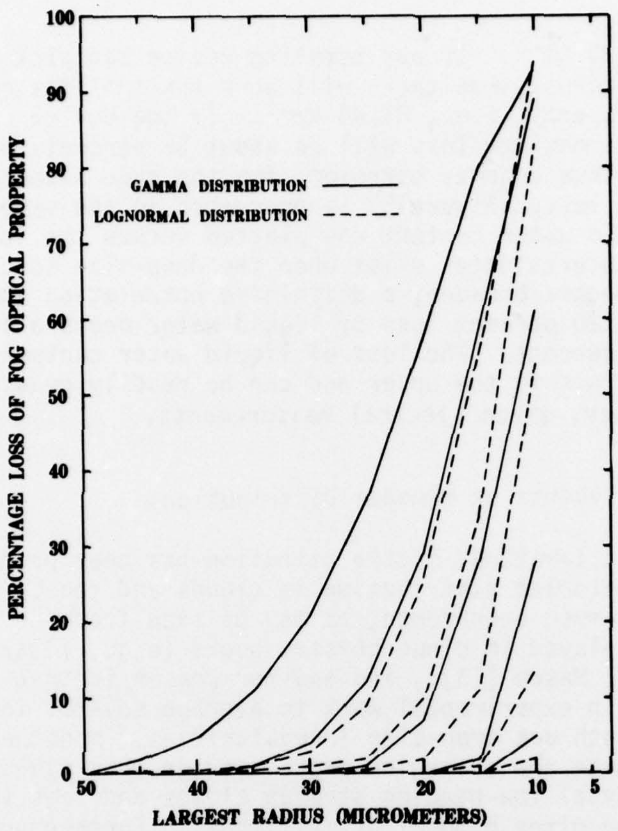

Figure 9. Percentage loss of optical property (or extinction coefficient) as a result of sampling restrictions or errors in upper tail end of a drop-size distribution.

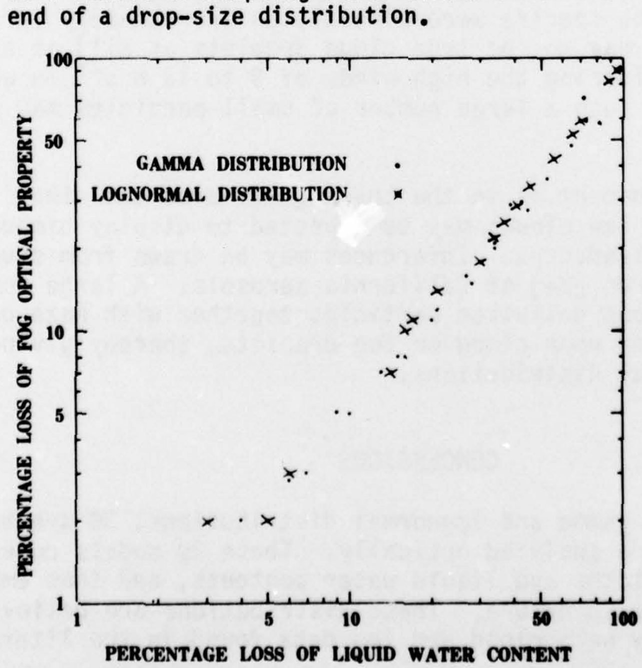

Figure 10. Percentage loss of optical property (or extinction coefficient) as a function of the percentage loss of liquid water content.

An excellent correlation was discovered between cloud liquid water and visual extinction derived therefrom. This correlation appears to be quite independent of drop-size spectral width. Microphysical and visibility data from several diverse sources in the literature were used (despite their limitations) in an attempt to test the utility of such theoretical correlation. As a result, the more appropriate conclusions are:

The regression line derived from such correlation (β versus w) which can be scaled upward or downward, may serve as a standard to gauge the departure of observed drop-size spectra from a unimodal distribution.

When a drop-size distribution is known to be unimodal or nearly so, (i) either liquid water or spectral extinction may be estimated from the regression line, given the other; (ii) the quality of observed microphysical and spectral data may be assessed against this line; and (iii) increasing or decreasing the liquid water content (or the droplet number concentration) will produce a corresponding change of the extinction coefficient without regard to spectral shapes.

The transmission characteristics of the three spectral regions in the presence of clouds or fogs can be readily found from figs. 1, 2, and 3 together. In general, when the liquid water content is of the order of 0.05 g m^{-3} (narrow drop-size spectrum), the 10.5μm region is the best (minimum extinction) and the 3.75μm region the worst. When the liquid water content is of the order of 0.50 g m^{-3} (broad), the 10.5μm still enjoys a slight advantage over the 3.75μm, but the visible is better than either. When the liquid water content is of the order of 1.0 g m^{-3} or more (very broad), the visible is the best and the 10.5μm the worst.

The drop-size spectra of most clouds, nearly all radiation fogs, and many advection-radiation fogs may be considered unimodal, and hence the foregoing observations are applicable.

In the case of bimodal spectra such as may be found in orographic clouds and advection fogs, the regression line would give erroneous information. However, the regression line apparently may be used to provide some ball-park values if one is not averse to a 50 percent error.

Finally, while in theory there is little doubt that this convenient regression line or the so-called "scaling law" as represented by (10), (11), or (12) is applicable to all unimodal drop-size spectra having the statistical characteristics of the gamma and lognormal distribution functions, variations therefrom will occur in actual practice, mainly due to sampling errors and partially due to a failure to recognize the capricious nature of fog and cloud. Nevertheless, the fog data collected by the Atmospheric Sciences Laboratory at Meppen, Germany, in the spring of 1978 and at Fort Ord, California, in the fall of 1978 will be examined in the light of this theoretical or generalized relationship between extinction and liquid water content in order to determine the suitability of (10), (11), and (12) for incorporation in the Electro-Optical Systems Atmospheric Effects Library.

REFERENCES

1. Trabert, W., 1901, "Die Extinction des Lichtes in einem trüben Medium," Meteor. Z. 18:518-525.

2. aufm Kampe, H. J., and H. K. Weickmann, 1952, "Trabert's Formula and the Determination of the Water Content in Clouds," J. Meteorol., 9:167-171.

3. Houghton, H. G., and W. H. Radford, 1938, "On the Measurement of Drop Size and Liquid Water Content in Fogs and Clouds," Paps. Phys. Ocean. and Meteorol. 6(4), M.I.T., 31 pp.

4. Eldridge, R. G., 1966, "Haze and Fog Aerosol Distributions," J. Atmospheric Sci. 23:605-613

5. Arnulf, A., and J. Bricard, 1957, "Transmission by Haze and Fog in the Spectral Region 0.35 to 10 Microns," J. Opt. Soc. Am. 47:491-498.

6. Platt, C. M. R., 1970, "Transmission of Submillimeter Waves Through Water Clouds and Fogs," J. Atmospheric Sci. 27:421-425.

7. Kumai, M., 1973, "Arctic Fog Droplet Size Distribution and Its Effect on Light Attenuation," J. Atmospheric Sci. 30:635-643.

8. Carrier, L. W., G. A. Cato, and K. J. von Essen, 1967, "The Backscattering and Extinction of Visible and Infrared Radiation by Selected Major Cloud Models," Appl. Opt. 6:1209-1216.

9. Deirmendjian, D., 1969, Electromagnetic Scattering on Spherical Polydispersions, American Elsevier, 290 pp.

10. Fletcher, N. H., 1962, The Physics of Rainclouds, Cambridge University Press, 386 pp.

11. Borovikov, A. M., and A. Kh. Khrgian et al., 1963, Cloud Physics, Israel Program for Scientific Translations, 392 pp.

12. Jiusto, J. E., 1964, "Project Fog Drops: Investigation of Warm Fog Properties and Fog Modification Concepts," CAL Report RM-1788-P-4 (NASA CR-72), Cornell Aeronautical Laboratory, Buffalo, NY, 54 pp.

13. Mason, B. J., 1971, The Physics of Clouds, Oxford University Press, London, 671 pp.

14. van de Hulst, H. C., 1957, Light Scattering by Small Particles, John Wiley, 470 pp.

15. Johnson, J. C., 1954, Physical Meteorology, John Wiley, 393 pp.

16. Levin, L. M., 1958, "Functions to Represent Drop Size Distributions in Clouds," Izv. Geofiz. Ser. 10:1211-1221. (translation)

17. Garland, J. A., 1971, "Some Fog Droplet Size Distributions Obtained by an Impaction Method," Quart. J. Roy. Meteorol. Soc. 97:483-494.

18. Mack, E. J., and R. J. Pilié, 1973, "The Microstructure of Radiation Fog at Travis Air Force Base," Sci Report No. 2 (CJ-5076-M-2, AFCRL-TR-73-0609), Calspan Corp., Buffalo, NY, 63 pp.

19. Middleton, W. E. K., 1952, Vision Through the Atmosphere, University of Toronto Press, 250 pp.

20. Eldridge, R. G., 1971, "The Relationship Between Visibility and Liquid Water Content in Fogs," J. Atmospheric Sci. 28:1183-1186.

21. Squires, P., 1958, "The Microstructure and Colloidal Stability of Warm Clouds: I. The Relation Between Structure and Stability," Tellus, 10:256-261.

22. Ludwig, F. L., and E. Robinson, 1969, "Condensation Nuclei and Aerosol Populations Related to Fog Formation," SRI Project PSU-6676 Report, Stanford Res. Inst., 54 pp.

23. Eldridge, R. G., 1957, "Measurements of Cloud Drop-Size Distributions," J. Meteorol. 14:55-59.

24. Whitby, K. T., and G. M. Sverdrup, 1978, "California Aerosols: Their Physical and Chemical Characteristics," Particle Technology Laboratory, Publication No. 347, University of Minnesota, 44 pp.

DISTRIBUTION LIST

Dr. Frank D. Eaton
Geophysical Institute
University of Alaska
Fairbanks, AK 99701

Commander
US Army Aviation Center
ATTN: ATZQ-D-MA
Fort Rucker, AL 36362

Chief, Atmospheric Sciences Div
Code ES-81
NASA
Marshall Space Flight Center,
AL 35812

Commander
US Army Missile R&D Command
ATTN: DRDMI-CGA (B. W. Fowler)
Redstone Arsenal, AL 35809

Redstone Scientific Information Center
ATTN: DRDMI-TBD
US Army Missile R&D Command
Redstone Arsenal, AL 35809

Commander
US Army Missile R&D Command
ATTN: DRDMI-TEM (R. Haraway)
Redstone Arsenal, AL 35809

Commander
US Army Missile R&D Command
ATTN: DRDMI-TRA (Dr. Essenwanger)
Redstone Arsenal, AL 35809

Commander
HQ, Fort Huachuca
ATTN: Tech Ref Div
Fort Huachuca, AZ 85613

Commander
US Army Intelligence Center & School
ATTN: ATSI-CD-MD
Fort Huachuca, AZ 85613

Commander
US Army Yuma Proving Ground
ATTN: Technical Library
Bldg 2100
Yuma, AZ 85364

Naval Weapons Center (Code 3173)
ATTN: Dr. A. Shlanta
China Lake, CA 93555

Sylvania Elec Sys Western Div
ATTN: Technical Reports Library
PO Box 205
Mountain View, CA 94040

Geophysics Officer
PMTC Code 3250
Pacific Missile Test Center
Point Mugu, CA 93042

Commander
Naval Ocean Systems Center (Code 4473)
ATTN: Technical Library
San Diego, CA 92152

Meteorologist in Charge
Kwajalein Missile Range
PO Box 67
APO San Francisco, 96555

Director
NOAA/ERL/APCL R31
RB3-Room 567
Boulder, CO 80302

Library-R-51-Tech Reports
NOAA/ERL
320 S. Broadway
Boulder, CO 80302

National Center for Atmos Research
NCAR Library
PO Box 3000
Boulder, CO 80307

B. Girardo
Bureau of Reclamation
E&R Center, Code 1220
Denver Federal Center, Bldg 67
Denver, CO 80225

National Weather Service
National Meteorological Center
W321, WWB, Room 201
ATTN: Mr. Quiroz
Washington, DC 20233

Mil Assistant for Atmos Sciences
Ofc of the Undersecretary of Defense
for Rsch & Engr/E&LS - Room 3D129
The Pentagon
Washington, DC 20301

Defense Communications Agency
Technical Library Center
Code 205
Washington, DC 20305

Director
Defense Nuclear Agency
ATTN: Technical Library
Washington, DC 20305

HQDA (DAEN-RDM/Dr. de Percin)
Washington, DC 20314

Director
Naval Research Laboratory
Code 5530
Washington, DC 20375

Commanding Officer
Naval Research Laboratory
Code 2627
Washington, DC 20375

Dr. J. M. MacCallum
Naval Research Laboratory
Code 1409
Washington, DC 20375

The Library of Congress
ATTN: Exchange & Gift Div
Washington, DC 20540
2

Head, Atmos Rsch Section
Div Atmospheric Science
National Science Foundation
1800 G. Street, NW
Washington, DC 20550

CPT Hugh Albers, Exec Sec
Interdept Committee on Atmos Science
National Science Foundation
Washington, DC 20550

Director, Systems R&D Service
Federal Aviation Administration
ATTN: ARD-54
2100 Second Street, SW
Washington, DC 20590

ADTC/DLODL
Eglin AFB, FL 32542

Naval Training Equipment Center
ATTN: Technical Library
Orlando, FL 32813

Det 11, 2WS/OI
ATTN: Maj Orondorff
Patrick AFB, FL 32925

USAFETAC/CB
Scott AFB, IL 62225

HQ, ESD/TOSI/S-22
Hanscom AFB, MA 01731

Air Force Geophysics Laboratory
ATTN: LCB (A. S. Carten, Jr.)
Hanscom AFB, MA 01731

Air Force Geophysics Laboratory
ATTN: LYD
Hanscom AFB, MA 01731

Meteorology Division
AFGL/LY
Hanscom AFB, MA 01731

US Army Liaison Office
MIT-Lincoln Lab, Library A-082
PO Box 73
Lexington, MA 02173

Director
US Army Ballistic Rsch Lab
ATTN: DRDAR-BLB (Dr. G. E. Keller)
Aberdeen Proving Ground, MD 21005

Commander
US Army Ballistic Rsch Lab
ATTN: DRDAR-BLP
Aberdeen Proving Ground, MD 21005

Director
US Army Armament R&D Command
Chemical Systems Laboratory
ATTN: DRDAR-CLJ-I
Aberdeen Proving Ground, MD 21010

Chief CB Detection & Alarms Div
Chemical Systems Laboratory
ATTN: DRDAR-CLC-CR (H. Tannenbaum)
Aberdeen Proving Ground, MD 21010

Commander
Harry Diamond Laboratories
ATTN: DELHD-CO
2800 Powder Mill Road
Adelphi, MD 20783

Commander
ERADCOM
ATTN: DRDEL-AP
2800 Powder Mill Road
Adelphi, MD 20783
2

Commander
ERADCOM
ATTN: DRDEL-CG/DRDEL-DC/DRDEL-CS
2800 Powder Mill Road
Adelphi, MD 20783

Commander
ERADCOM
ATTN: DRDEL-CT
2800 Powder Mill Road
Adelphi, MD 20783

Commander
ERADCOM
ATTN: DRDEL-EA
2800 Powder Mill Road
Adelphi, MD 20783

Commander
ERADCOM
ATTN: DRDEL-PA/DRDEL-ILS/DRDEL-E
2800 Powder Mill Road
Adelphi, MD 20783

Commander
ERADCOM
ATTN: DRDEL-PAO (S. Kimmel)
2800 Powder Mill Road
Adelphi, MD 20783

Chief
Intelligence Materiel Dev & Support Ofc
ATTN: DELEW-WL-I
Bldg 4554
Fort George G. Meade, MD 20755

Acquisitions Section, IRDB-D823
Library & Info Service Div, NOAA
6009 Executive Blvd
Rockville, MD 20852

Naval Surface Weapons Center
White Oak Library
Silver Spring, MD 20910

The Environmental Research
Institute of MI
ATTN: IRIA Library
PO Box 8618
Ann Arbor, MI 48107

Mr. William A. Main
USDA Forest Service
1407 S. Harrison Road
East Lansing, MI 48823

Dr. A. D. Belmont
Research Division
PO Box 1249
Control Data Corp
Minneapolis, MN 55440

Director
Naval Oceanography & Meteorology
NSTL Station
Bay St Louis, MS 39529

Director
US Army Engr Waterways Experiment Sta
ATTN: Library
PO Box 631
Vicksburg, MS 39180

Environmental Protection Agency
Meteorology Laboratory
Research Triangle Park, NC 27711

US Army Research Office
ATTN: DRXRO-PP
PO Box 12211
Research Triangle Park, NC 27709

Commanding Officer
US Army Armament R&D Command
ATTN: DRDAR-TSS Bldg 59
Dover, NJ 07801

Commander
HQ, US Army Avionics R&D Activity
ATTN: DAVAA-O
Fort Monmouth, NJ 07703

Commander/Director
US Army Combat Surveillance & Target Acquisition Laboratory
ATTN: DELCS-D
Fort Monmouth, NJ 07703

Commander
US Army Electronics R&D Command
ATTN: DELCS-S
Fort Monmouth, NJ 07703

US Army Materiel Systems Analysis Activity
ATTN: DRXSY-MP
Aberdeen Proving Ground, MD 21005

Director
US Army Electronics Technology & Devices Laboratory
ATTN: DELET-D
Fort Monmouth, NJ 07703

Commander
US Army Electronic Warfare Laboratory
ATTN: DELEW-D
Fort Monmouth, NJ 07703

Commander
US Army Night Vision & Electro-Optics Laboratory
ATTN: DELNV-L (Dr. Rudolf Buser)
Fort Monmouth, NJ 07703

Commander
ERADCOM Technical Support Activity
ATTN: DELSD-L
Fort Monmouth, NJ 07703

Project Manager, FIREFINDER
ATTN: DRCPM-FF
Fort Monmouth, NJ 07703

Project Manager, REMBASS
ATTN: DRCPM-RBS
Fort Monmouth, NJ 07703

Commander
US Army Satellite Comm Agency
ATTN: DRCPM-SC-3
Fort Monmouth, NJ 07703

Commander
ERADCOM Scientific Advisor
ATTN: DRDEL-SA
Fort Monmouth, NJ 07703

6585 TG/WE
Holloman AFB, NM 88330

AFWL/WE
Kirtland, AFB, NM 87117

AFWL/Technical Library (SUL)
Kirtland AFB, NM 87117

Commander
US Army Test & Evaluation Command
ATTN: STEWS-AD-L
White Sands Missile Range, NM 88002

Rome Air Development Center
ATTN: Documents Library
TSLD (Bette Smith)
Griffiss AFB, NY 13441

Commander
US Army Tropic Test Center
ATTN: STETC-TD (Info Center)
APO New York 09827

Commandant
US Army Field Artillery School
ATTN: ATSF-CD-R (Mr. Farmer)
Fort Sill, OK 73503

Commandant
US Army Field Artillery School
ATTN: ATSF-CF-R
Fort Sill, OK 73503

Director CFD
US Army Field Artillery School
ATTN: Met Division
Fort Sill, OK 73503

Commandant
US Army Field Artillery School
ATTN: Morris Swett Library
Fort Sill, OK 73503

Commander
US Army Dugway Proving Ground
ATTN: MT-DA-L
Dugway, UT 84022

Dr. C. R. Sreedrahan
Research Associates
Utah State University, UNC 48
Logan, UT 84322

Inge Dirmhirn, Professor
Utah State University, UNC 48
Logan, UT 84322

Defense Documentation Center
ATTN: DDC-TCA
Cameron Station Bldg 5
Alexandria, VA 22314
12

Commanding Officer
US Army Foreign Sci & Tech Center
ATTN: DRXST-IS1
220 7th Street, NE
Charlottesville, VA 22901

Naval Surface Weapons Center
Code G65
Dahlgren, VA 22448

Commander
US Army Night Vision
& Electro-Optics Lab
ATTN: DELNV-D
Fort Belvoir, VA 22060

Commander and Director
US Army Engineer Topographic Lab
ETL-TD-MB
Fort Belvoir, VA 22060

Director
Applied Technology Lab
DAVDL-EU-TSD
ATTN: Technical Library
Fort Eustis, VA 23604

Department of the Air Force
OL-C, 5WW
Fort Monroe, VA 23651

Department of the Air Force
5WW/DN
Langley AFB, VA 23665

Director
Development Center MCDEC
ATTN: Firepower Division
Quantico, VA 22134

US Army Nuclear & Chemical Agency
ATTN: MONA-WE
Springfield, VA 22150

Director
US Army Signals Warfare Laboratory
ATTN: DELSW-OS (Dr. R. Burkhardt)
Vint Hill Farms Station
Warrenton, VA 22186

Commander
US Army Cold Regions Test Center
ATTN: STECR-OP-PM
APO Seattle, WA 98733

Dr. John L. Walsh
Code 5560
Navy Research Lab
Washington, DC 20375

Commander
TRASANA
ATTN: ATAA-PL
(Dolores Anguiano)
White Sands Missile Range, NM 88002

Commander
US Army Dugway Proving Ground
ATTN: STEDP-MT-DA-M (Mr. Paul Carlson)
Dugway, UT 84022

Commander
US Army Dugway Proving Ground
ATTN: STEDP-MT-DA-T
(Mr. William Peterson)
Dugway, UT 84022

Commander
USATRADOC
ATTN: ATCD-SIE
Fort Monroe, VA 23651

Commander
USATRADOC
ATTN: ATCD-CF
Fort Monroe, VA 23651

Commander
USATRADOC
ATTN: Tech Library
Fort Monroe, VA 23651

ATMOSPHERIC SCIENCES RESEARCH PAPERS

1. Lindberg, J.D., "An Improvement to a Method for Measuring the Absorption Coefficient of Atmospheric Dust and other Strongly Absorbing Powders," ECOM-5565, July 1975.
2. Avara, Elton, P., "Mesoscale Wind Shears Derived from Thermal Winds," ECOM-5566, July 1975.
3. Gomez, Richard B., and Joseph H. Pierluissi, "Incomplete Gamma Function Approximation for King's Strong-Line Transmittance Model," ECOM-5567, July 1975.
4. Blanco, A.J., and B.F. Engebos, "Ballistic Wind Weighting Functions for Tank Projectiles," ECOM-5568, August 1975.
5. Taylor, Fredrick J., Jack Smith, and Thomas H. Pries, "Crosswind Measurements through Pattern Recognition Techniques," ECOM-5569, July 1975.
6. Walters, D.L., "Crosswind Weighting Functions for Direct-Fire Projectiles," ECOM-5570, August 1975.
7. Duncan, Louis D., "An Improved Algorithm for the Iterated Minimal Information Solution for Remote Sounding of Temperature," ECOM-5571, August 1975.
8. Robbiani, Raymond L., "Tactical Field Demonstration of Mobile Weather Radar Set AN/TPS-41 at Fort Rucker, Alabama," ECOM-5572, August 1975.
9. Miers, B., G. Blackman, D. Langer, and N. Lorimier, "Analysis of SMS/GOES Film Data," ECOM-5573, September 1975.
10. Manquero, Carlos, Louis Duncan, and Rufus Bruce, "An Indication from Satellite Measurements of Atmospheric CO2 Variability," ECOM-5574, September 1975.
11. Petracca, Carmine, and James D. Lindberg, "Installation and Operation of an Atmospheric Particulate Collector," ECOM-5575, September 1975.
12. Avara, Elton P., and George Alexander, "Empirical Investigation of Three Iterative Methods for Inverting the Radiative Transfer Equation," ECOM-5576, October 1975.
13. Alexander, George D., "A Digital Data Acquisition Interface for the SMS Direct Readout Ground Station — Concept and Preliminary Design," ECOM-5577, October 1975.
14. Cantor, Israel, "Enhancement of Point Source Thermal Radiation Under Clouds in a Nonattenuating Medium," ECOM-5578, October 1975.
15. Norton, Colburn, and Glenn Hoidale, "The Diurnal Variation of Mixing Height by Month over White Sands Missile Range, N.M," ECOM-5579, November 1975.
16. Avara, Elton P., "On the Spectrum Analysis of Binary Data," ECOM-5580, November 1975.
17. Taylor, Fredrick J., Thomas H. Pries, and Chao-Huan Huang, "Optimal Wind Velocity Estimation," ECOM-5581, December 1975.
18. Avara, Elton P., "Some Effects of Autocorrelated and Cross-Correlated Noise on the Analysis of Variance," ECOM-5582, December 1975.
19. Gillespie, Patti S., R.L. Armstrong, and Kenneth O. White, "The Spectral Characteristics and Atmospheric CO2 Absorption of the Ho^{+3}:YLF Laser at 2.05μm," ECOM-5583, December 1975.
20. Novlan, David J. "An Empirical Method of Forecasting Thunderstorms for the White Sands Missile Range," ECOM-5584, February 1976.
21. Avara, Elton P., "Randomization Effects in Hypothesis Testing with Autocorrelated Noise," ECOM-5585, February 1976.
22. Watkins, Wendell R., "Improvements in Long Path Absorption Cell Measurement," ECOM-5586, March 1976.
23. Thomas, Joe, George D. Alexander, and Marvin Dubbin, "SATTEL — An Army Dedicated Meteorological Telemetry System," ECOM-5587. March 1976.
24. Kennedy, Bruce W., and Delbert Bynum, "Army User Test Program for the RDT&E-XM-75 Meteorological Rocket," ECOM-5588, April 1976.

25. Barnett, Kenneth M., "A Description of the Artillery Meteorological Comparisons at White Sands Missle Range, October 1974 - December 1974 ('PASS' - Prototype Artillery [Meteorological] Subsystem)," ECOM-5589, April 1976.
26. Miller, Walter B., "Preliminary Analysis of Fall-of-Shot From Project 'PASS'," ECOM-5590, April 1976.
27. Avara, Elton P., "Error Analysis of Minimum Information and Smith's Direct Methods for Inverting the Radiative Transfer Equation," ECOM-5591, April 1976.
28. Yee, Young P., James D. Horn, and George Alexander, "Synoptic Thermal Wind Calculations from Radiosonde Observations Over the Southwestern United States," ECOM-5592, May 1976.
29. Duncan, Louis D., and Mary Ann Seagraves, "Applications of Empirical Corrections to NOAA-4 VTPR Observations," ECOM-5593, May 1976.
30. Miers, Bruce T., and Steve Weaver, "Applications of Meterological Satellite Data to Weather Sensitive Army Operations,"ECOM-5594, May 1976.
31. Sharenow, Moses, "Redesign and Improvement of Balloon ML-566," ECOM-5595, June, 1976.
32. Hansen, Frank V., "The Depth of the Surface Boundary Layer," ECOM-5596, June 1976.
33. Pinnick, R.G., and E.B. Stenmark, "Response Calculations for a Commercial Light-Scattering Aerosol Counter," ECOM-5597, July 1976.
34. Mason, J., and G.B. Hoidale, "Visibility as an Estimator of Infrared Transmittance," ECOM-5598, July 1976.
35. Bruce, Rufus E., Louis D. Duncan, and Joseph H. Pierluissi, "Experimental Study of the Relationship Between Radiosonde Temperatures and Radiometric-Area Temperatures," ECOM-5599, August 1976.
36. Duncan, Louis D., "Stratospheric Wind Shear Computed from Satellite Thermal Sounder Measurements," ECOM-5800, September 1976.
37. Taylor, F., P. Mohan, P. Joseph and T. Pries, "An All Digital Automated Wind Measurement System," ECOM-5801, September 1976.
38. Bruce, Charles, "Development of Spectrophones for CW and Pulsed Radiation Sources," ECOM-5802, September 1976.
39. Duncan, Louis D., and Mary Ann Seagraves,"Another Method for Estimating Clear Column Radiances," ECOM-5803, October 1976.
40. Blanco, Abel J., and Larry E. Taylor, "Artillery Meteorological Analysis of Project Pass," ECOM-5804, October 1976.
41. Miller, Walter, and Bernard Engebos," A Mathematical Structure for Refinement of Sound Ranging Estimates," ECOM-5805, November, 1976.
42. Gillespie, James B., and James D. Lindberg, "A Method to Obtain Diffuse Reflectance Measurements from 1.0 to 3.0 μm Using a Cary 17I Spectrophotometer," ECOM-5806, November 1976.
43. Rubio, Roberto, and Robert O. Olsen,"A Study of the Effects of Temperature Variations on Radio Wave Absorption,"ECOM-5807, November 1976.
44. Ballard, Harold N., "Temperature Measurements in the Stratosphere from Balloon-Borne Instrument Platforms, 1968-1975," ECOM-5808, December 1976.
45. Monahan, H.H., "An Approach to the Short-Range Prediction of Early Morning Radiation Fog," ECOM-5809, January 1977.
46. Engebos, Bernard Francis, "Introduction to Multiple State Multiple Action Decision Theory and Its Relation to Mixing Structures," ECOM-5810, January 1977.
47. Low, Richard D.H.,"Effects of Cloud Particles on Remote Sensing from Space in the 10-Micrometer Infrared Region," ECOM-5811, January 1977.
48. Bonner, Robert S., and R. Newton, "Application of the AN/GVS-5 Laser Rangefinder to Cloud Base Height Measurements," ECOM-5812, February 1977.
49. Rubio, Roberto, "Lidar Detection of Subvisible Reentry Vehicle Erosive Atmospheric Material," ECOM-5813, March 1977.
50. Low, Richard D.H., and J.D. Horn, "Mesoscale Determination of Cloud-Top Height: Problems and Solutions," ECOM-5814, March 1977.

51. Duncan, Louis D., and Mary Ann Seagraves, "Evaluation of the NOAA-4 VTPR Thermal Winds for Nuclear Fallout Predictions," ECOM-5815, March 1977.
52. Randhawa, Jagir S., M. Izquierdo, Carlos McDonald and Zvi Salpeter, "Stratospheric Ozone Density as Measured by a Chemiluminescent Sensor During the Stratcom VI-A Flight," ECOM-5816, April 1977.
53. Rubio, Roberto, and Mike Izquierdo, "Measurements of Net Atmospheric Irradiance in the 0.7- to 2.8-Micrometer Infrared Region," ECOM-5817, May 1977.
54. Ballard, Harold N., Jose M. Serna, and Frank P. Hudson Consultant for Chemical Kinetics, "Calculation of Selected Atmospheric Composition Parameters for the Mid-Latitude, September Stratosphere," ECOM-5818, May 1977.
55. Mitchell, J.D., R.S. Sagar, and R.O. Olsen, "Positive Ions in the Middle Atmosphere During Sunrise Conditions," ECOM-5819, May 1977.
56. White, Kenneth O., Wendell R. Watkins, Stuart A. Schleusener, and Ronald L. Johnson, "Solid-State Laser Wavelength Identification Using a Reference Absorber," ECOM-5820, June 1977.
57. Watkins, Wendell R., and Richard G. Dixon, "Automation of Long-Path Absorption Cell Measurements," ECOM-5821, June 1977.
58. Taylor, S.E., J.M. Davis, and J.B. Mason, "Analysis of Observed Soil Skin Moisture Effects on Reflectance," ECOM-5822, June 1977.
59. Duncan, Louis D. and Mary Ann Seagraves, "Fallout Predictions Computed from Satellite Derived Winds," ECOM-5823. June 1977.
60. Snider, D.E., D.G. Murcray, F.H. Murcray, and W.J. Williams, "Investigation of High-Altitude Enhanced Infrared Backround Emissions" (U), SECRET, ECOM-5824, June 1977.
61. Dubbin, Marvin H. and Dennis Hall, "Synchronous Meteorlogical Satellite Direct Readout Ground System Digital Video Electronics," ECOM-5825, June 1977.
62. Miller, W., and B. Engebos, "A Preliminary Analysis of Two Sound Ranging Algorithms," ECOM-5826, July 1977.
63. Kennedy, Bruce W., and James K. Luers, "Ballistic Sphere Techniques for Measuring Atomspheric Parameters," ECOM-5827, July 1977.
64. Duncan, Louis D., "Zenith Angle Variation of Satellite Thermal Sounder Measurements," ECOM-5828, August 1977.
65. Hansen, Frank V., "The Critical Richardson Number," ECOM-5829, September 1977.
66. Ballard, Harold N., and Frank P. Hudson (Compilers), "Stratospheric Composition Balloon-Borne Experiment," ECOM-5830, October 1977.
67. Barr, William C., and Arnold C. Peterson, "Wind Measuring Accuracy Test of Meteorological Systems," ECOM-5831, November 1977.
68. Ethridge, G.A. and F.V. Hansen, "Atmospheric Diffusion: Similarity Theory and Empirical Derivations for Use in Boundary Layer Diffusion Problems," ECOM-5832, November 1977.
69. Low, Richard D.H., "The Internal Cloud Radiation Field and a Technique for Determining Cloud Blackness," ECOM-5833, December 1977.
70. Watkins, Wendell R., Kenneth O. White, Charles W. Bruce, Donald L. Walters, and James D. Lindberg, "Measurements Required for Prediction of High Energy Laser Transmission," ECOM-5834, December 1977.
71. Rubio, Robert, "Investigation of Abrupt Decreases in Atmospherically Backscattered Laser Energy," ECOM-5835. December 1977.
72. Monahan, H.H. and R.M. Cionco, "An Interpretative Review of Existing Capabilities for Measuring and Forecasting Selected Weather Variables (Emphasizing Remote Means)," ASL-TR-0001, January 1978.
73. Heaps, Melvin G., "The 1979 Solar Eclipse and Validation of D-Region Models," ASL-TR-0002. March 1978.

74. Jennings, S.G., and J.B. Gillespie, "M.I.E. Theory Sensitivity Studies - The Effects of Aerosol Complex Refractive Index and Size Distribution Variations on Extinction and Absorption Coefficients Part II: Analysis of the Computational Results," ASL-TR-0003, March 1978.

75. White, Kenneth O. et al, "Water Vapor Continuum Absorption in the 3.5μm to 4.0μm Region," ASL-TR-0004, March 1978.

76. Olsen, Robert O., and Bruce W. Kennedy, "ABRES Pretest Atmospheric Measurements," ASL-TR-0005, April 1978.

77. Ballard, Harold N., Jose M. Serna, and Frank P. Hudson, "Calculation of Atmospheric Composition in the High Latitude September Stratosphere," ASL-TR-0006, May 1978.

78. Watkins, Wendell R. et al, "Water Vapor Absorption Coefficients at HF Laser Wavelengths," ASL-TR-0007, May 1978.

79. Hansen, Frank V., "The Growth and Prediction of Nocturnal Inversions," ASL-TR-0008, May 1978.

80. Samuel, Christine, Charles Bruce, and Ralph Brewer, "Spectrophone Analysis of Gas Samples Obtained at Field Site," ASL-TR-0009, June 1978.

81. Pinnick, R.G. et al., "Vertical Structure in Atmospheric Fog and Haze and its Effects on IR Extinction," ASL-TR-0010, July 1978.

82. Low, Richard D.H., Louis D. Duncan, and Richard B. Gomez, "The Microphysical Basis of Fog Optical Characterization," ASL-TR-0011, August 1978.

83. Heaps, Melvin G., "The Effect of a Solar Proton Event on the Minor Neutral Constituents of the Summer Polar Mesosphere," ASL-TR-0012, August 1978.

84. Mason, James B., "Light Attenuation in Falling Snow," ASL-TR-0013, August 1978.

85. Blanco, Abel J., "Long-Range Artillery Sound Ranging: "PASS" Meteorological Application," ASL-TR-0014, September 1978.

86. Heaps, M.G., and F.E. Niles, "Modeling the Ion Chemistry of the D-Region: A case Study Based Upon the 1966 Total Solar Eclipse," ASL-TR-0015, September 1978.

87. Jennings, S.G., and R.G. Pinnick, "Effects of Particulate Complex Refractive Index and Particle Size Distribution Variations on Atmospheric Extinction and Absorption for Visible Through Middle-Infrared Wavelengths," ASL-TR-0016, September 1978.

88. Watkins, Wendell R., Kenneth O. White, Lanny R. Bower, and Brian Z. Sojka, " Pressure Dependence of the Water Vapor Continuum Absorption in the 3.5- to 4.0-Micrometer Region," ASL-TR-0017, September 1978.

89. Miller, W.B., and B.F. Engebos, "Behavior of Four Sound Ranging Techniques in an Idealized Physical Enviroment," ASL-TR-0018, September 1978.

90. Gomez, Richard G., "Effectiveness Studies of the CBU-88/B Bomb, Cluster, Smoke Weapon" (U), CONFIDENTIAL ASL-TR-0019, September 1978.

91. Miller, August, Richard C. Shirkey, and Mary Ann Seagraves, "Calculation of Thermal Emission from Aerosols Using the Doubling Technique," ASL-TR-0020, November, 1978.

92. Lindberg, James D. et al., "Measured Effects of Battlefield Dust and Smoke on Visible, Infrared, and Millimeter Wavelengths Propagation: A Preliminary Report on Dusty Infrared Test-I (DIRT-I)," ASL-TR-0021, January 1979.

93. Kennedy, Bruce W., Arthur Kinghorn, and B.R. Hixon, "Engineering Flight Tests of Range Meteorological Sounding System Radiosonde," ASL-TR-0022, February 1979.

94. Rubio, Roberto, and Don Hoock, "Microwave Effective Earth Radius Factor Variability at Wiesbaden and Balboa," ASL-TR-0023, February 1979.

95. Low, Richard D.H., "A Theoretical Investigation of Cloud/Fog Optical Properties and Their Spectral Correlations," ASL-TR-0024, February 1979.

☆U.S. GOVERNMENT PRINTING OFFICE: 1979 677-017/30